DOI: 10.1534/genetics.108.090563

Note

Efficient Ends-Out Gene Targeting In Drosophila

Juan Huang,*[,1] Wenke Zhou,*[,1] Annie M. Watson,* Yuh-Nung Jan[†] and Yang Hong*[,2]

**Department of Cell Biology and Physiology, University of Pittsburgh School of Medicine, Pittsburgh, Pennsylvania 15261 and [†]Howard Hughes Medical Institute, Departments of Physiology and Biochemistry, University of California, San Francisco, California 94143*

Manuscript received April 22, 2008
Accepted for publication June 14, 2008

ABSTRACT

In this report, we describe several approaches to improve the scalability and throughput of major genetic crosses in ends-out gene targeting. We generated new sets of targeting vectors and fly stocks and introduced a novel negative selection marker that drastically reduced the frequency of false-positive targeting candidates.

THE development of homologous recombination-based gene targeting is a landmark breakthrough in Drosophila genetics (Rong and Golic 2000; Gong and Golic 2003). In particular, the so-called "ends-out" or replacement-type gene targeting offers a straightforward approach for generating either knockout or knockin alleles. To date, there are already >20 genes that have been modified by ends-out targeting (supplemental Table 1). Nonetheless, the frequency of target-specific homologous recombination in Drosophila varies tremendously, ranging from >1/200 gametes (Manoli *et al.* 2005) to <1/350,000 (Jones *et al.* 2007) (also Y. Hong, unpublished data), *i.e.*, a >1800-fold difference. In cases of low targeting efficiency (<1/100,000 gametes), ends-out targeting can be exceedingly time and labor intensive. Here, we optimized the current ends-out targeting scheme by focusing on improving the scalability and throughput of its major genetic crosses. As illustrated in Figure 1a, there are three major genetic crosses in a typical ends-out targeting. In the targeting cross, virgin females of a transgenic line bearing the donor DNA ("*P{donor}*") are crossed with *hs-FLP, hs-I-SceI* males, and their larval progeny are heat-shocked to induce the generation of linear donor DNA fragments by FLPase and I-SceI enzymes. In the screening cross, virgin females from the targeting cross that are of the correct genotype (*P{donor}*/hs-FLP, hs-I-SceI*) are crossed with proper chromosome balancer males, and preliminary targeting candidates are recovered on the basis of their w^+ marker. However, many of these candidates might be false positives due to the failure of excision or non-targeting integration of the donor DNA. In the mapping cross, only preliminary candidates whose w^+ marker is mapped to the target gene chromosome are selected for further analysis.

For the targeting cross, the number of *P{donor}*/hs-FLP, hs-I-SceI* virgin females directly determines the scale of the whole targeting experiment. Genes that are resistant to homologous recombination may require collecting and sorting >15,000 virgins from the targeting cross (Larsson *et al.* 2004), which is extremely labor intensive due to the time-sensitive nature of virgin collection and the genotyping process. To eliminate this major bottleneck in scaling up the targeting cross, we modified the original *hs-FLP, hs-I-SceI* stocks by replacing their Y chromosomes and balancer chromosomes with ones that contain *hs-hid* transgenes (Grether *et al.* 1995). We named these modified stocks "6934-hid" and "6935-hid" (Figure 1b) after the original stock numbers. Ubiquitous expression of the cell-death gene *hid* induced by heat shock causes strong lethality. As illustrated in Figure 1c, in a targeting cross using 6934-hid, all male progeny and those female progeny carrying *hs-hid* balancer chromosome are eliminated. Since *P{donor}*/hs-FLP, hs-I-SceI* females are the only genotype that survives, 6934-hid and 6935-hid completely eliminate the time-sensitive virgin collection and genotyping process.

For screening and mapping crosses, we found their throughput was often severely limited by the high background of false positives, which may represent >95–99.9% of preliminary candidates (J. Huang, W. Zhou, and Y. Hong, unpublished results, and see below). Therefore, we introduced a negative selection marker into the current ends-out targeting scheme, so the

[1]These authors contributed equally to this article.

[2]*Corresponding author:* Department of Cell Biology and Physiology, University of Pittsburgh School of Medicine, S325 BST, 3500 Terrace St., Pittsburgh, PA 15261. E-mail: yhong@pitt.edu

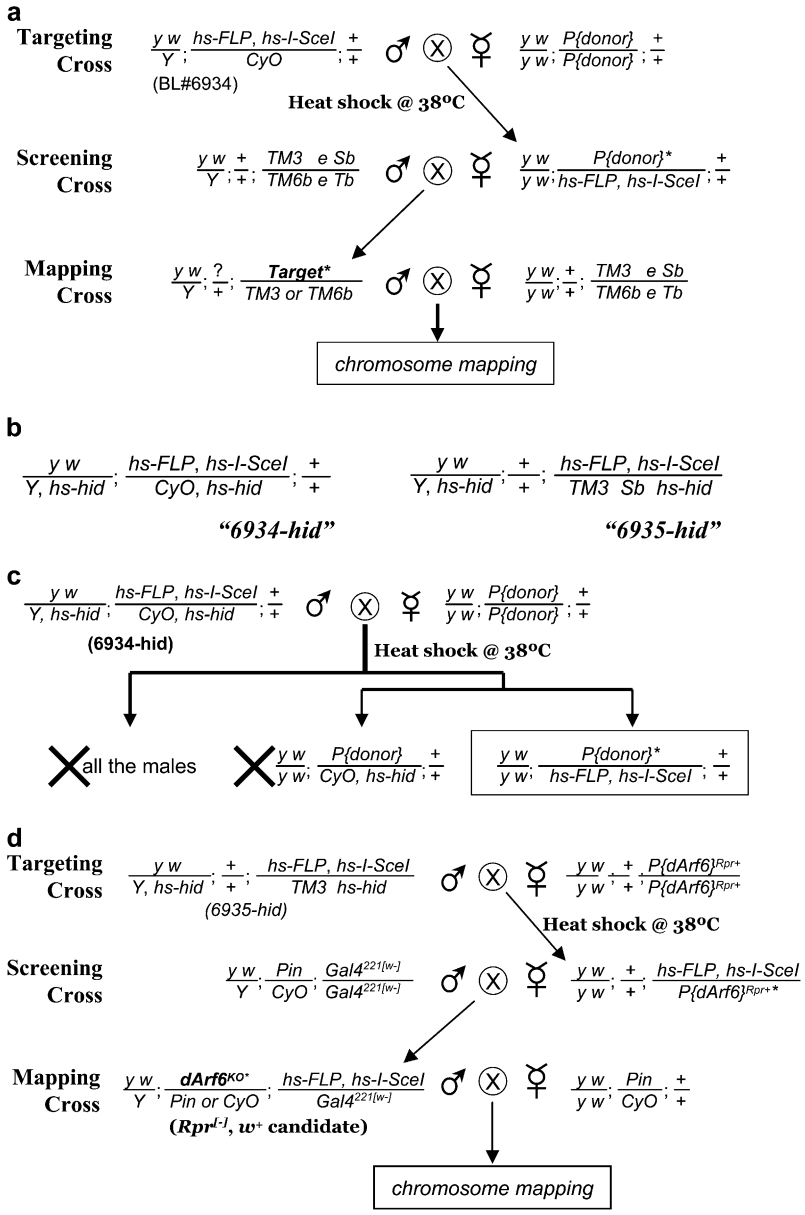

FIGURE 1.—Genetic crosses in targeting experiments. (a) Genetic crosses of a typical ends-out targeting experiment. The transgenic donor DNA ("*P{donor}*") is on the second chromosome, while the target gene is on the third chromosome. *P{donor}**, linearized extrachromosomal donor DNA fragment that only exists transiently—it will either be lost permanently or inserted into a chromosome by targeted or nontargeted integration events. *Target**, potential targeting events. Note that the majority of potential targeting events may be nonspecific and not located on the third chromosome (see text). ?, this copy of the second chromosome is inherited from the female in the screening cross. It could be the donor chromosome or *hs-FLP, hs-I-SceI*, or the recombinant between the two. Nonetheless, this copy of the chromosome is irrelevant in the mapping cross. (b) Genotypes of 6934-hid and 6935-hid. (c) 6934-hid stock eliminates the virgin collection and genotype sorting in the targeting cross. (d) The genetic cross scheme of the $dArf6^{KO}$ targeting experiment. Because *dArf6* is on the second chromosome, a transgenic line carrying $dArf6^{KO}$ donor DNA ("$P\{dArf6\}^{Rpr+}$") on the third chromosome was used. *w; Pin/CyO; Gal4*$^{221[w-]}$ stock was used to set up the screening cross in lieu of a regular *Pin/CyO* balancer stock. This allowed simultaneous selection against nonspecific targeting candidates while balancing the potential specific targeting candidates from the screening cross. $P\{dArf6\}^{Rpr+}$*, linearized extrachromosomal $dArf6^{KO}$ donor DNA fragment. $dArf6^{KO}$*, potential targeting events.

majority of nontargeted integrations may be directly eliminated before they are subject to any further screening and mapping efforts. Ectopic expression of another cell-death gene *reaper* (*rpr*), similar to *hid*, also causes strong lethality (WHITE *et al.* 1996). As illustrated in Figure 2b, a *UAS-Rpr* module can be tagged to the 3′ end of a transgenic donor DNA fragment (*e.g.*, $P\{crb::mEosFP^{KI}\}$). Once the donor DNA fragment is recombined into the target gene locus, *UAS-Rpr* will be lost due to homologous recombination. In contrast, nontargeted integrations will likely retain the donor DNA fragment with an intact *UAS-Rpr* module ("Rpr^+"). By using proper *Gal4* driver stocks to set up the screening cross, Rpr^+ / *Gal4* false-positive candidates will be directly eliminated due to the ectopic expression of Rpr.

To implement the *UAS-Rpr* selection, we made a new set of ends-out targeting vectors, pRK1 and pRK2 (Figure 2a) that were based on the integration and modification of pEndsOut2 and pBS70W (available from http://dgrc.cgb.indiana.edu/). Both pRK1 and pRK2 contain a *UAS-Rpr* module, while pRK2 also has a GMR (HAY *et al.* 1994)-enhanced w^+ marker to further facilitate the recovery of targeting candidates. We made two targeting constructs, a $crb::mEosFP^{KI}$ knockin construct (Figure 2b) and a $dArf6^{KO}$ knockout construct (Figure 2c), on the basis of pRK1 and pRK2, respectively. Crb is a transmembrane protein essential for developing cell polarity (TEPASS *et al.* 1990). We plan to study the trafficking and dynamics of Crb by tagging it with a photoconvertible fluorescent protein mEosFP (WIEDENMANN *et al.* 2004). *dArf6 (Arf51F)* is a small GTPase that may play key roles in Drosophila muscle and nervous system development, although no *dArf6* mutants are currently available. $dArf6^{KO}$ targeting aims to delete 2.158 kb of the

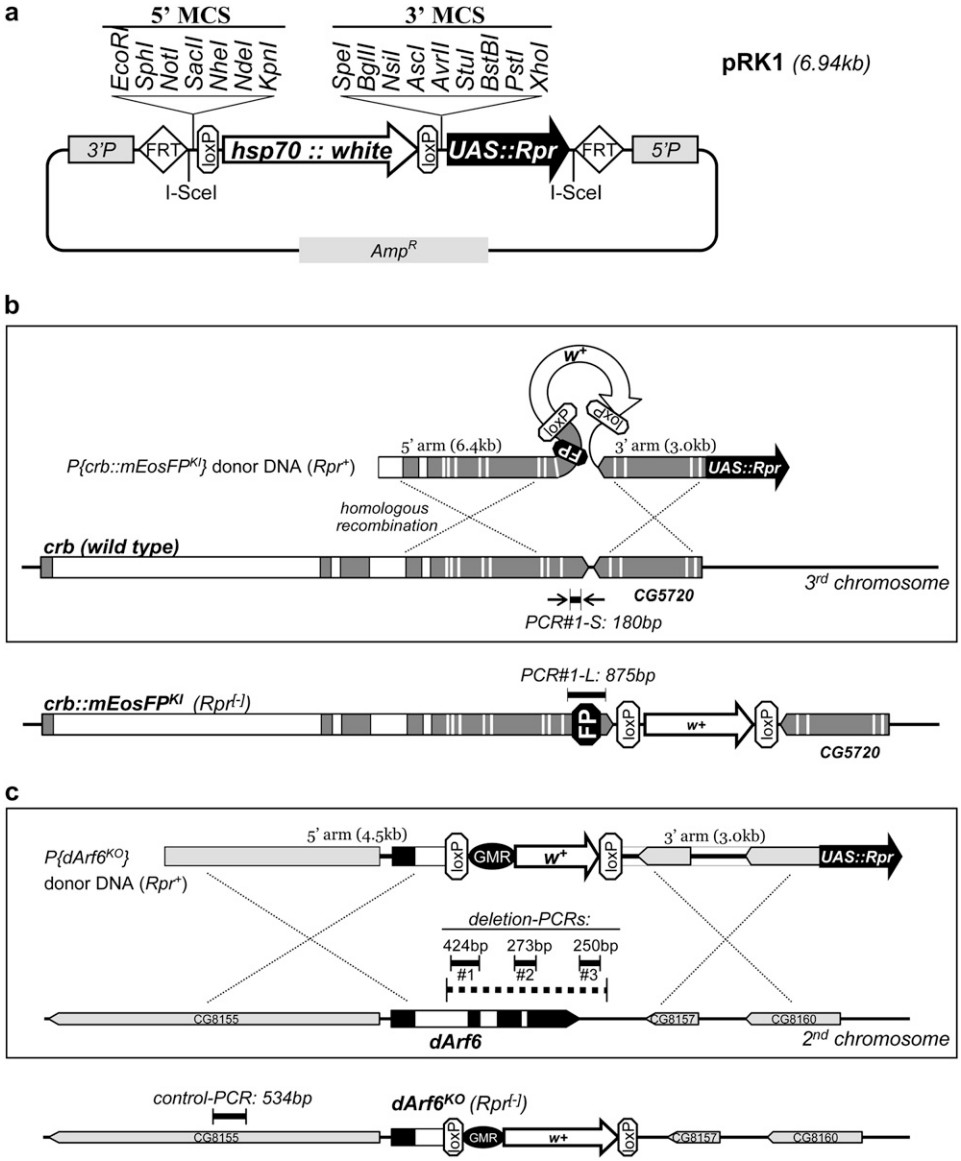

FIGURE 2.—pRK1 vector and targeting of *crb::mEosFP*^{KI} and *dArf6*^{KO}. (a) Only pRK1 is diagrammed here. The *hsp70::white* (*w*$^{+}$) transformation marker is flanked by two loxP sites so that *w*$^{+}$ can be removed in the final targeted alleles by Cre recombinase. *MCS*, multiple cloning sites. *Amp*^{R}, ampicillin-resistant gene. *3′P* and *5′P*, 3′ and 5′ *P*-element sequences for transgenic insertion. (b) *crb::mEosFP*^{KI} knockin targeting. mEosFP ("FP") is fused in frame at the position right outside the transmembrane domain of Crb. (c) *dArf6*^{KO} knockout targeting. Dotted bar indicates the targeted deletion (2.158 kb). In both b and c, shaded or solid boxes are exons and open boxes are introns (introns and exons are not shown for CG8155, CG8157, and CG8160 in c). Fine dotted lines indicate the homologous recombination event. Solid bars indicate the positions and sizes of diagnostic and verification PCRs (for PCR results please see supplemental Figures 1 and 2). Diagrams are not precisely to scale.

dArf6 locus that includes all the coding exons plus the 3′-UTR (Figure 2c). We obtained multiple transgenic lines from both targeting constructs at normal frequency (supplemental Table 2), indicating that *UAS-Rpr* in pRK1 and pRK2 was sufficiently silent in the absence of the Gal4 driver and did not adversely affect the routine *P*-element-based transgenic process. All the transgenic donor lines were larval or pupal lethal when crossed with neuronal-specific drivers *Gal4*^{477} and *Gal4*^{221} (supplemental Table 2) (GRUEBER *et al.* 2003). *Gal4*^{221}/*UAS-Rpr* also consistently produced very few adult escapers of a fully penetrated wing inflation phenotype (supplemental Figure 1d).

To evaluate the effectiveness of *UAS-Rpr* without any bias, we first carried out *crb::mEosFP*^{KI} knockin experiments without *UAS-Rpr* selection (similar to Figure 1a). From $\sim 5 \times 10^4$ screening cross progenies, we recovered 270 male candidates, of which 14 were mapped to the third chromosome where *crb* is located. We then screened 125 non-third chromosome candidates and all 14 third chromosome candidates for the presence of *UAS-Rpr* by crossing them into *Gal4*^{221}. As summarized in Table 1, only 3/125 of the non-third chromosome candidates (*i.e.*, false positives) are *Rpr*$^{[-1]}$,while 11/14 of the third chromosome candidates are *Rpr*$^{[-1]}$ of which 7 were confirmed by PCR to have the correct targeting events (supplemental Figure 1a). Extrapolating from these data, selecting against *UAS-Rpr* in the screening cross of *crb::mEosFP*^{KI} would eliminate >96% (253/263) of false positives (Table 1). In addition, UAS-Rpr selection also eliminates tandem-insertion mutants (GONG and GOLIC 2003), which can be difficult to distinguish from true targeting candidates by simple PCR assays (supplemental Figure 1, b and c). The homologous recombination frequency of *crb::mEosFP*^{KI} is $\sim$1/7000 if only considering the male candidates.

We then decided to carry out a large-scale *dArf6*^{KO} targeting experiment by taking full advantage of the new

TABLE 1

Genetic and PCR analyses of targeting candidates of *crb::mEosFP^{KI}* and *dArf6^{KO}*

Targeted allele	Targeting candidates	*Rpr* test	*FRT*$^+$	*loxP*$^+$	X chr	PCR verified
crb::mEosFP^{KI}	Non-third chr candidates	*Rpr*$^+$ 122	17/122	122/122	0/122	ND
		Rpr$^{[-]}$ 3	0/3	3/3	0/3	ND
	Third chr candidates	*Rpr*$^+$ 3	0/3	3/3	—	2[a]/3
		Rpr$^{[-]}$ 11	0/11	11/11	—	7/11
dArf6^{KO}[b]	Non-second chr candidates	*Rpr*$^+$ 120	54/120	ND	0/120	ND
		Rpr$^{[-]}$ 2	0/2	ND	0/2	ND
	Second chr candidates	*Rpr*$^+$ 2	0/2	ND	—	ND
		Rpr$^{[-]}$ 0	—	—	—	—

Rpr$^+$, scored by lethality or strong wing phenotypes in the presence of *Gal4$^{221[w-]}$* or *Gal4$^{477[w-]}$*. The total number of *Rpr*$^{[-]}$ false positives of *crb::mEosFP^{KI}* can be estimated as 10 [6 from non-third chromosome candidates ($3 \times (256/125)$], plus 4 from third chromosome candidates). *FRT*$^+$ or *loxP*$^+$, scored by eye color variegation in the presence of constitutively expressed FLPase or Cre recombinase. Approximately 87% [$(263 - (17 \times 2))/263$] of *crb::mEosFP^{KI}* false positives and ~57% [$(124 - 54)/124$] of *dArf6^{KO}* false positives showed damaged FRT sites. X chr, candidates that were mapped to the X chromosome. Here, none of the nontarget chromosome false positives were mapped to the X chromosome. Since the 4th chromosome is extremely small, therefore unlikely to harbor any nonspecific targeting events, "X chr" data indicate that virtually all of the nontarget chromosome false positives retained their donor DNA on the original chromosome, due to either damaged FRT sites or insufficient excision of donor DNA. ND, not done; —, not applicable.

[a] Tandem insertion mutants.

[b] Only *dArf6^{KO}* candidates recovered from screening crosses with regular *Pin/CyO* balancer stock are listed here (see Table 2).

reagents and methods described here, as we failed at *dArf6^{KO}* targeting on the basis of the original pEndsOut2 vector by screening ~1.6×10^5 screening cross progenies (W. Zhou and Y. Hong, unpublished results). We recloned the same 5′ and 3′ homologous arms into the pRK2-based vector. By using 6935-hid to set up the targeting cross, we easily collected $>2 \times 10^4$ virgin females. Twelve thousand of them were mated with *w/Y; Pin/CyO; Gal4$^{221[w-]}$* males to set up the screening cross (Figure 1d). From $>7 \times 10^5$ screening cross progenies (Table 2) we recovered 315 *w*$^+$ males, of which 5 were verified as specific targeting candidates by PCR (Table 2, supplemental Figure 2, a and b). As a control, 200 virgin females from the same targeting cross were crossed with regular *w/Y, Pin/CyO* males. Of 124 *w*$^+$ male candidates recovered, 1.6% (2/124) were *Rpr*$^{[-]}$, but none harbored the true targeting event (Tables 1 and 2). Thus, *UAS-Rpr* selection achieved an impressive ~60-fold reduction of false positives. Effectively, *dArf6^{KO}* targeting was accomplished at a scale equivalent to screening/mapping >18,000 (315×60) preliminary candidates in the absence of *UAS-Rpr* selection. In addition, the dramatically reduced number of preliminary candidates, combined with their dark-red eye color due to GMR-enhanced *w*$^+$ expression in pRK2, made the screening process much easier and faster. The homologous recombination frequency of *dArf6^{KO}* can be estimated as ~1/140,000 if only considering the male candidates. Homozygotes of *dArf6^{KO}* are viable but are male and female sterile, so it is possible that *dArf6* only plays a specific and indispensable role in germline development. When we were preparing this article, a *P*-element-induced deletion allele of dArf6 was published and Dyer *et al.* (2007) observed the same male and female sterile phenotypes in their homozygous *dArf6* mutant flies.

Compared with the "rapid scheme" in which preliminary candidates were screened for the loss of FRT sites (Rong *et al.* 2002; Gong and Golic 2003), *UAS-Rpr* selection is more efficient since it directly eliminates false positives. In addition, we found that the majority of the false positives (57–87%) had damaged FRT sites (Table 1); therefore, they could only be eliminated by *UAS-Rpr* selection but not by the FRT test. Since the *I-SceI* sites are positioned rather close to the FRT sites in ends-out targeting constructs, we speculate that the frequent FRT damage seen here was most likely due to the double-strand DNA repair process triggered by the premature cut of *I-SceI* sites (Bellaiche *et al.* 1999; Gong and

TABLE 2

***dArf6^{KO}* targeting with and without using *UAS-Rpr* as a negative selection marker**

Screening cross set up	Progenies screened	Male candidates	Second chr candidates	*Rpr*$^+$	*FRT*$^+$	PCR verified
(×) *w/Y; Pin/CyO; Gal4$^{221[w-]}$*	$>7 \times 10^5$	315	30/315	—	ND	5/30
(×) *w/Y; Pin/CyO*	~7300	124	2[a]/124	122/124	54/124	ND

chr, chromosome; ND, not done; —, not applicable.

[a] These two candidates harbored nontargeted integration of donor DNA on the second chromosome and were *Rpr*$^+$.

Golic 2003). Separating FRT and *I-SceI* sites further away in future pRK-based targeting vectors should further reduce the frequency of false positives. Consistently, the Golic lab reported that the frequency of false positives was low using the pW25 targeting vector in which FRT and *I-SceI* were separated by 100–150 bp (Gong and Golic 2004). Since pRK-based vectors may not be suitable for making Gal4 knockin alleles, pW25 series vectors should be excellent alternatives.

In summary, for a targeting experiment with an expected homologous recombination frequency of ~1/100,000 gametes, we estimate that our 6934-hid/6935-hid stocks and UAS-Rpr selection reduced the work load of genetic crosses to a level comparable to a routine *P*-excision experiment. In addition, our new targeting vectors, such as pRK2, should significantly facilitate the molecular cloning and transgenesis of targeting constructs due to the enhanced multiple cloning sites and w^+ expression. Overall, these new reagents and methods should significantly increase the success rate of targeting experiments on genes that are resistant to homologous recombination.

We are grateful to Jeff Sekelsky for pBS70W and pEndsOut2 plasmids, Leon Perniciaro for help in screening in *dArf6*^{KO} targeting candidates, Ulrich Nienhaus for EosFP constructs, Fabrice Rogers for hs-hid stocks, and Fen-Biao Gao, Sige Zou, Peizhang Xu, and Koen Venken for comments on the manuscript. Y.N.J is an investigator of the Howard Hughes Medical Institute. pRK1 and pRK2 will be donated to the Drosophila Genomic Resource Center (DGRC) and 6934-hid and 6935-hid stocks will be donated to the Bloomington Stock Center. This work is supported by start-up funds from the University of Pittsburgh School of Medicine (Y.H.).

LITERATURE CITED

Bellaiche, Y., V. Mogila and N. Perrimon, 1999 I-SceI endonuclease, a new tool for studying DNA double-strand break repair mechanisms in Drosophila. Genetics **152:** 1037–1044.

Dyer, N., E. Rebollo, P. Dominguez, N. Elkhatib, P. Chavrier *et al.*, 2007 Spermatocyte cytokinesis requires rapid membrane addition mediated by ARF6 on central spindle recycling endosomes. Development **134:** 4437–4447.

Gong, W. J., and K. G. Golic, 2003 Ends-out, or replacement, gene targeting in Drosophila. Proc. Natl. Acad. Sci. USA **100:** 2556–2561.

Gong, W. J., and K. G. Golic, 2004 Genomic deletions of the Drosophila melanogaster Hsp70 genes. Genetics **168:** 1467–1476.

Grether, M. E., J. M. Abrams, J. Agapite, K. White and H. Steller, 1995 The head involution defective gene of Drosophila melanogaster functions in programmed cell death. Genes Dev. **9:** 1694–1708.

Grueber, W. B., L. Y. Jan and Y. N. Jan, 2003 Different levels of the homeodomain protein cut regulate distinct dendrite branching patterns of Drosophila multidendritic neurons. Cell **112:** 805–818.

Hay, B. A., T. Wolff and G. M. Rubin, 1994 Expression of baculovirus P35 prevents cell death in Drosophila. Development **120:** 2121–2129.

Jones, W. D., P. Cayirlioglu, I. G. Kadow and L. B. Vosshall, 2007 Two chemosensory receptors together mediate carbon dioxide detection in Drosophila. Nature **445:** 86–90.

Larsson, M. C., A. I. Domingos, W. D. Jones, M. E. Chiappe, H. Amrein *et al.*, 2004 Or83b encodes a broadly expressed odorant receptor essential for Drosophila olfaction. Neuron **43:** 703–714.

Manoli, D. S., M. Foss, A. Villella, B. J. Taylor, J. C. Hall *et al.*, 2005 Male-specific fruitless specifies the neural substrates of Drosophila courtship behaviour. Nature **436:** 395–400.

Rong, Y. S., and K. G. Golic, 2000 Gene targeting by homologous recombination in Drosophila. Science **288:** 2013–2018.

Rong, Y. S., S. W. Titen, H. B. Xie, M. M. Golic, M. Bastiani *et al.*, 2002 Targeted mutagenesis by homologous recombination in D. melanogaster. Genes Dev. **16:** 1568–1581.

Tepass, U., C. Theres and E. Knust, 1990 crumbs encodes an EGF-like protein expressed on apical membranes of Drosophila epithelial cells and required for organization of epithelia. Cell **61:** 787–799.

White, K., E. Tahaoglu and H. Steller, 1996 Cell killing by the Drosophila gene reaper. Science **271:** 805–807.

Wiedenmann, J., S. Ivanchenko, F. Oswald, F. Schmitt, C. Rocker *et al.*, 2004 EosFP, a fluorescent marker protein with UV-inducible green-to-red fluorescence conversion. Proc. Natl. Acad. Sci. USA **101:** 15905–15910.

Communicating editor: J. A. Lopez

SUPPLEMENTARY INFORMATION

SUPPLEMENTARY MATERIALS AND METHODS

Fly stocks and genetics: The following stocks were obtained from the Bloomington stock center:
BL#6934: *y^1 w; P{70FLP}11 P{70I-SceI}2B noc^{Sco}/CyO*
BL#6935: *y^1 w; P{70FLP}23 P{70I-SceI}4A /TM6*
BL#6938: *w^{1118}; P{70FLP}10*
BL#8846:, *y^1 w; Dp(2;Y)G, P{hs-hid}Y*
BL#1557: *y w; Bl^1 L^2 / CyO, P{hs-hid}4*
BL#1558: *y w; Pr^1 Dr^1 / TM3, P{hs-hid}14, Sb*
BL#766: *y^1 w^{67c23} P{Crey}1b; noc^{Sco}/CyO*
BL#851: *y^1 w^{67c23} P{Crey}1b; D*/TM3, Sb*
All transgenic flies were created using *w^{1118}* stocks via the standard *P*-elements-based transgenic protocol. Most fly cultures and crosses were carried out at room temperature (~22ºC) or 25ºC. Crosses for generating 6934-hid and 6935-hid stocks were carried out entirely under 18ºC to minimize the potential leaky expression of *hs-hid*. However, we found that 6934-hid and 6935-hid can be readily maintained at room temperature, although for long-term stock maintenance, we recommend 18ºC. Males of *Y.hs-hid* are slightly weaker due to having two copies of *hs-hid* genes, so culturing stocks under 25ºC is not recommended. It is important to keep vials and bottles from being overcrowded since *Y.hs-hid* males may not survive very well under crowded conditions. An average bottle of 6934-hid yields >150 males, while for 6935-hid, > 250 males can be expected from a bottle in good conditions. In targeting crosses using 6934-hid or 6935-hid, a few non-disjunction (XO) males were observed in rare cases, but they were all sterile (M. van Doren, personal communication to FlyBase; http://flybase.org/reports/FBrf0089994.html). *P{70FLP} P{70I-SceI (i.e., hs-FLP, hs-I-SceI*) chromosomes from BL#6934 and BL#6935 are homozygous-viable, but cannot be maintained as homozygous stocks.

Gene Targeting: Gene targeting experiments were carried out as described (GONG and GOLIC 2003) with the following modifications. All transgenic donor lines were pre-screened/validated as shown in Supplementary Table 2. Transgenic donor lines with the best FRT-excision efficiency, strongest *UAS-Rpr* expression (judged by lethality), and carrying the donor DNA insertion on the non-target chromosomes were used for targeting (Supplementary Table 2). In the targeting cross, we set up 20-40 vials (25x95mm) of crosses. Each vial contained 25-30 virgin females of transgenic donor flies mated with 25-40 *6934-hid* or *6935-hid* males. It is highly recommended to use young and fresh males of *6934-hid* or *6935-hid*. Crosses were maintained under room temperature and flies were transferred to new vials every 24 hours. Eggs in transferred vials were aged under 25°C, and were heat-shocked at day 2 (*i.e.,* 24-48 hours after egg-laying) and day 3 (*i.e.,* 48-72 hours after egg-laying), respectively. Heat shock was carried out under 38ºC for 60-90 minutes in a 20-liter circulating water bath. Based on our experiences, an extra heat-shock at day 3 (96-120 hours after egg-laying) does not seem to be essential, as there were no significant differences in eye color variegation in females from the targeting cross with double or triple heat-shock treatments – the excision was nearly 100% in both cases as judged by eye color variegation. In the screening cross, ten virgin females from the targeting crosses were mated with five proper balancer males in each vial. Flies were transferred to fresh vials every couple of days under either room temperature or 25°C. With a total of five transfers, each screening cross routinely produced >1000 progeny from five vials. Preliminary targeting

candidates from targeting crosses were screened based on eye color. In the mapping cross, a single male candidate was crossed with proper balancer virgin females. All female candidates were discarded because they required an extra round of cross to be mapped. Due to the large number of flies screened, we did not strictly follow the origin of each candidate so we could not comment on the clonality of these candidates.

Generation of *Gal4$^{221[w-]}$* and *Gal4$^{477[w-]}$* lines via imprecise P-element excision: Because original *Gal4^{221}* and *Gal4^{477}* stocks carry the *w^{+}* marker, they cannot be used directly to substitute balancer stocks in the screening crosses. Both *Gal4^{221}* and *Gal4^{477}* are *P*-element based Gal4-trap lines (GRUEBER *et al.* 2003), so we converted them to *w$^{[-]}$* by screening imprecise excision events that specifically removed the *w^{+}* marker but not the Gal4. 29% (12/42) of *Gal4^{221}* and 27% (3/11) of *Gal4^{477} w$^{[-]}$* excision lines retained the original Gal4 insertion, which were confirmed by GFP expression patterns by crossing into *UAS-mCD8::GFP* stock (GRUEBER *et al.* 2003). When crossed into pRK1 or pRK2 based transgenic lines (Supplementary Table 2) and *Rpr+* non-specific targeting candidates, these lines showed lethality or wing inflation phenotypes indistinguishable from original *Gal4^{477}* or *Gal4^{221}*. We then further constructed new balancer stocks *w; Pin/CyO; Gal4$^{221[w-]}$* and *w; Gal4$^{477[w-]}$; TM2 e Ubx/TM6b e Tb* that are suitable for simultaneously selecting against *UAS-Rpr* and balancing the target candidates in the screening crosses.

Primers:

MCS#1-5':
AGGTCTCAGTACGAATTCTTGCATGCAATGCGGCCGCTACCGCGGGCTAGCACATATGCAG
GTACCATAACTTCGTATAATGTATGCTATACGAAGTTATCGTACGCCATG
MCS#1-3':
GCGTACGATAACTTCGTATAGCATACATTATACGAAGTTATGGTACCTGCATATGTGCTAGCC
CGCGGTAGCGGCCGCATTGCATGCAAGAATTCGTACTGAGACCTGC
MCS#2-5':
TCGACACCGGTATAACTTCGTATAATGTATGCTATACGAAGTTATCACTAGTAAAGATCTCCA
TGCATAAGGCGCGCCTAGGCCTATTCGAATCTGCAGCTCGAGC
MCS#2-3':
GTACGCTCGAGCTGCAGATTCGAATAGGCCTAGGCGCGCCTTATGCATGGAGATCTTTACTA
GTGATAACTTCGTATAGCATACATTATACGAAGTTATACCGGTG
YH505: CGTTACACCCTTGCTCAAGTC
YH609: GTCATG TCTAGA GCTAGC AGTGCGA TTAAGCCAGA C
YH630: GTCATG CTCGAG ACTAGT TCG TCT GGC ATT GTC AGG C
YH631: ATCAGC GCGGCCGC GCCTAGCGAACAGGCATGGCTAAAA TCGCCAATGC GTCAC
YH632: ATCAGC CTCGAG GCTAGC GGAGCCATTA AAGTACGCCT CCTTC
YH633: ATCAGC CTCGAG GCTAGC TCGACCACAG ACATTGCCAT CATTGTAATA
YH634: ATCAGC GGTACC TCTAGA GCAAAATATG TTTTTTATTT GATTTAC
YH635: ATCAGC GCG GCCGCTG GTGACTTAGG ATTAGTTTGT TAC
YH636: ATCAGC GAATTC GGATGCATTA CCTCCATTTA AGACTACTT
YH637: ATCAGC GAATTC GTAATGCATC CTTGTTTTGA AACATCA
YH638: ATCAGC CTCGAG GCTAGC AGGCCCGTCC TCCTTGGCCG TAATCTG
YH639: ATCAGC ACTAGT ATGCAT GTATCTAAGC GTAAACTTAA GAGACTGTAC
YH640: ATCAGC CTCGAG ACTACTATCG GTGTTAACCG GCAAAAAGAC
YH663: ATCAGCGGTACCTCTAGAATGGCAGTGGCATTCTACATAC
YH664: ATCAGCCTGCAGTCATTGCGATGGCTTGCGATATTTG
YH665: TCCCAAGGAT GCATTATTAT TGATTAAGG
YH666: ATCAGC GCGGCCGC GTCGAC GATTAACC GTTAGTTTAG CAAGTATAAT TG
YH667: ATCAGC GCGGCCGC CTCGAG TGCAGGTCGG
YH668: CACTTTACTG CAGATTGTTT AGC
YH669: AACA ATATGCATTA AAGTGCAAGT TAAAGTG

YH670: TCA GAATTC TCTAGA GCCTGTTCGCTAGGC CAATTCCCTATTCAG
HJ58: AACCGGACTACTACTGCGAGTG
HJ59: TATTACAATGATGGCAATGTCTGTG
HJ91: GTAACAAACTAATCCTAAGTCACCAGC
HJ92: GTCTTTTTGCCGGTTAACACCG
WK50: CGAGATGCGGCCGCGTATTCACTGCACTGACTCCATTAAG
WK51: CGAGATGGTACCAGGGTCAGTGAATTTCCAGATAATAG
WK77: CGAGATACTAGTTTTTGTGGGTGTATGTCTTGTTTTAT
WK82: TGGAGGTTTCGCCTTTGGT
WK84: CGAGATACTAGTGTTTTACAGATGAAAAGGTTGTGATG
WK87: CGAGATCTCGAGACCACTTATTTTTAAGGCCAATACAC
WK88: CGAGATGCGGCCGCGCCCTGAATCTCGCCCAGCTATTC
WK93: CGAGATGGTACCGTGACTCTACTAATTATTATATATTTTTATTATTATAATAC
WK119: AAGTTCTGCATAACACTCATCGAATA
WK126: TTCGATTAGTGATAGTACTGGTGTACG
WK139: CGAGATGCGGCCGCACTCTCAATTAACCAACCAATATTCTC

Construction of pRK1 and pRK2 vectors: To construct pRK1, we first made a targeting vector, pKIKO, without *UAS-Rpr*. Four long primers, MCS#1-5, MCS#1-3, MCS#2-5 and MCS#2-3, that bear the desired restriction enzyme sites and loxP sites, were synthesized. MCS#2-5 and MSC#2-3 were first annealed to form a double-stranded linker with *Acc65*I and *Xho*I/*Sal*I compatible ends at 5' and 3', respectively. It was then inserted into the sites between *Acc65*I and *Xho*I of pBS-70W to make an intermediate construct pBS-70W2 containing the loxP and MCS upstream of the *white*$^+$ marker. Both *Acc65*I*/Kpn*I and *Xho*I sites in the original pBS-70W were eliminated. Then, MCS#1-5 and MSC#1-3 were annealed to form a double-stranded linker with *Sac*II and *Sph*I compatible ends at 5' and 3', respectively. It was then inserted between the *Sac*II and *Sph*I sites of pBS-70W2. The whole fragment **"***Bsa*I + MCS#1 + loxP + *hsp70::white*$^+$ + loxP + MCS#2" was cut out with *BsaI* (which is designed to generate an *Acc65*I-compatible end) and *Xho*I and cloned into the sites between *Acc65*I and *Xho*I in pEndsOut2 to yield the final construct of pKIKO.

To make pRK1, the *UAS-Rpr*-Pros 3'UTR module was assembled first. The *Reaper* coding sequence was PCR amplified from genomic DNA using primers YH663 and YH664, cut with *Kpn*I and *Pst*I and cloned into the pBluescript vector to make pBlue-Rpr. The 3' UTR sequence of *pros29* (which encodes a 29 kDa unit of proteosome complex) was PCR amplified from genomic DNA with primers YH665 and YH666, cut with *Nsi*I and *Not*I and cloned into pBlue-Rpr to make pBlue-Rpr-3'UTR. A 250bp fragment of the 5' end of the UAS promoter was PCR amplified by YH667 and YH668 from the pUAST vector and cut with *BamH*I + *Pst*I, while a 150bp fragment of the 3' end of the UAS promoter was PCR amplified from the pUAST vector with YH669 and YH670, and cut with *Nsi*I and *EcoR*I. Both PCR fragments were then inserted between *Not*I and *EcoR*I of the pBluescript vector via three-factor ligation. The resulted pBlue-UAS contains a 400bp UAS promoter with a *numb* Kozak site at its 3' end to facilitate target gene expression. The Rpr+3'UTR fragment was then cut out from pBlue-Rpr-3'UTR with *Xba*I and *Sal*I and inserted into pBlue-UAS to make pBlue-*UAS-Rpr*-3'UTR. The whole ~890bp *UAS-Rpr*-3'UTR module was then cut with *Xho*I and *Sal*I and cloned into the *Xho*I site of pKIKO. Constructs with *UAS-Rpr*-3'UTR oriented properly (Fig. 2) were selected and named as pRK1. pRK2 was constructed by inserting a GMR (HAY *et al.* 1994) enhancer into the *Age*I site of pRK1, leaving only the 5' *Age*I site intact.

We purposely left two unique sites, *Bsi*W I and *Age*I, at each end of the *w*$^+$ marker in pKIKO, pRK1 and pRK2. These two sites are designed for future modifications of the vector should new features have to be added, *e.g.,* replacing the *w*$^+$

marker with a GFP marker, or replacing wild type loxP sites with other lox site variants. pRK2 was generated by adding GMR enhancer into the *BsiWI* site of pRK1. In addition, enzyme sites in 5' MCS are ordered similarly to the popular pUAST vector. Thus, when pRK1 or pRK2 is used for making knock-in constructs, such as generating GFP fusion alleles of a target gene, the same GFP tagged 5' gDNA can be readily cloned into the pUAST vector. Therefore, fusion protein expression and/or function can be validated by overexpression before the much more time-consuming knock-in process begins. Also, unlike *Gong & Golic 2004* (GONG and GOLIC 2004) we did not put any stop codons surrounding the loxP sites, since we imagine most knock-out designs will aim to delete a sufficient length of target gDNA, so inserting extra stop codons might not be necessary. Should such sequences be required, they can be easily inserted into the end of 5' or 3' MCS.

pRK1-Crb::mEosFP targeting construct: To assemble the 5' gDNA containing the Crumbs::mEosFP knock-in sequence in which mEosFP is inserted in frame right outside the transmembrane domain of Crumbs, we first made a pUAST-Crumbs-intra::mEosFP construct. In brief, a gDNA of 840bp encoding the transmembrane domain, the intracellular domain and the 3'UTR of crumbs up to the *Xba*I site (WODARZ *et al.* 1995) was PCR amplified from gDNA by YH633 and YH634, with the original *Xba*I site replaced by *Kpn*I. It was then cloned into pBluescript between *Xho*I and *Kpn*I to make pBlue-{YH633+634}. The first 96aa of the N-terminus of Crumbs, including the potential signal peptide, was PCR amplified with YH631 and YH632 from pUAS-Crb transgenic lines (WODARZ *et al.* 1995). YH632 is positioned the same as the Crb-1 primer in *Wodarz et al* but contains a *Nhe*I site instead of *Bgl*II. This 335bp PCR fragment was cut with *Not*I and *Xho*I and inserted into the *Not*I and *Xho*I sites of pBlue-{YH633+634}. This makes a so-called "Crumbs-intra" sequence (WODARZ *et al.* 1995) that contains the signal peptide, transmembrane domain and intracellular domain of Crumbs, with much of the extracellular domains deleted.

The mEosFP coding sequence was PCR amplified with YH609 and YH630 using pcDNA3-mEosFP (WIEDENMANN *et al.* 2004) as template, cut with *Nhe*I and *Spe*I, and inserted into pBlue-Crumbs-intra to make pBlue-Crumbs-intra::mEosFP in which mEosFP is inserted in-frame immediately before the transmembrane domain. This fragment was then cut with *Not*I and *Kpn*I and cloned into the pUAST vector to make pUAST-Crumbs-intra::mEosFP.

To make pRK1-Crumbs::mEosFP, the 3.0kb 3' gDNA starting from the *Xba*I site downstream of *Crumbs*' 3' UTR was first PCR amplified with YH639 and YH640, cut with *Spe*I and *Xho*I, and inserted into pRK1 between *Spe*I and *Xho*I to make pRK1-{YH639-640}. This 3' gDNA fragment covers the neighboring gene CG5720 and was confirmed to be free of PCR errors by sequencing both strands. The 4.9kb 5' gDNA sequence was pieced together by two PCR fragments amplified with the primers YH635+YH636 for the first 2.1kb, and YH637+YH638 for the second 2.8kb. The former was cut with *Not*I and *EcoR*I and cloned into pBluescript first, and then the latter was cloned in between the *EcoR*I and *Xho*I sites. This 5' gDNA, which ends before the original *Xba*I site, right outside the transmembrane domain of Crumbs, was cloned into pBlue-Crumbs-intra::mEosFP by *Not*I and *Xho*I digestion, replacing the first 96aa of Crumbs' N-terminus coding sequence. This fully assembled 5' gDNA arm of Crumbs::mEosFP was cloned into pRK1-{YH639-640} to make the final pRK1-Crumbs::mEosFP construct. All long-range PCR reactions were carried out using *PfuUltra*^{TM} DNA polymerase (STRATAGENE).

dArf6^{KO} targeting construct: To make pKIKO-dArf6^{KO}, a 4.5kb 5' gDNA arm was first PCR amplified with primers WK50 and WK51 from BAC clone RP98_33K6 (Children's Hospital, Oakland, California, USA), cut with *Not*I and *Acc65*I, and inserted into pRK2 between *Not*I and *Acc65*I to make pKIKO-{WK50-51}. Then, the 3.2 kb 3' gDNA arm was PCR amplified with the primers WK84 and WK87, cut with *Spe*I and *Xho*I, and inserted into pKIKO-{WK50-51} between *Spe*I and *Xho*I to make the final pKIKO-dArf6^{KO} targeting construct. Both 5' and 3' gDNA arms were confirmed to be free of PCR errors by sequencing both strands. The same arms were cloned from pKIKO-dArf6^{KO} into pRK2 to make pRK2-dArf6^{KO}. The 3' end of the 5' arm in pRK2-dArf6^{KO} was slightly modified to facilitate post-targeting modification of the *dArf6^{KO}* allele (W.Z. and Y.H., unpublished data).

Verification of *crb::mEosFP^{KI}* and *dArf6^{KO}* targeted alleles: To verify the *crb::mEosFP^{KI}* allele, genomic DNA was extracted from homozygous mutant larvae or adult males for PCR verification. HJ58 and HJ59 flank the mEosFP insertion in *crb::mEosFP^{KI}*. Wild type gDNA will yield a 185bp product, while gDNA from knock-in homozygous mutant larvae or adults will yield a much larger 875bp product due to insertion of mEosFP into the *crb* locus. To PCR verify the tandem insertion mutants, primers HJ91 and HJ92 were used (Fig. 3c), and a 1.0kb product was expected. To verify the *dArf6^{KO}* allele, genomic DNA was extracted from homozygous *dArf6^{KO}* mutant males. Deletion-PCR#2 (273bp) was first carried out using the primers WK139 and YH505, which are located at the middle of the deletion region. The deletion-PCR#2-negative candidates were verified again by two more PCRs; deletion-PCR#1 (424bp) with primers WK88 and WK126, and deletion-PCR#2 (250bp) with primers WK77 and WK93. These two pairs of primers are located at the 5' and 3' end of the targeted deletion, respectively. Homozygous lethal *dArf6^{KO}* candidate #7 was PCR-verified using a transheterozygous male by crossing with *dArf6$^{KO\#16}$*. For the control-PCR, primers WK82 and WK119, which are located far away from the deletion region, were used. They yielded a 534bp product. All samples should be positive for control-PCR. Wild-type and fake candidates are positive for all three deletion-PCRs, while homozygotes of *dArf6^{KO}* should be negative for all three deletion-PCRs. For each sample, control and diagnostic PCRs were always carried out simultaneously and were repeated at least twice to exclude random PCR failures.

SUPPLEMENTARY FIGURE LEGEND:

Supplementary Figure 1. Verification of *crb::mEosFP^{KI}* mutants.

a. Verification of *crb::mEosFP^{KI}* targeting candidates that were mapped to the 3rd chromosome. PCR primers are designed to flank the insertion of mEosFP in *crb::mEosFP^{KI}* allele (Fig. 2b). They amplify an 875bp PCR product (PCR#1L) that contains the mEosFP sequence from *crb::mEosFP^{KI}* genomic DNA or donor DNA, but a much smaller product of an 185bp (PCR#1S) from wild type genomic DNA. PCR from homozygous *crb::mEosFP^{KI}* mutants that contain no wild type *crb* alleles should be positive only for the PCR#1L product. Please note that non-specific candidates containing wild type *crb* alleles will show the PCR#1S product, but they could also be positive for PCR#1L because of the non-specific insertion of donor DNA on the 3rd chromosome. **: tandem insertion mutant that were Rpr^{+}*. #: *Rpr^{+}* without tandem insertion.

b. Tandem-insertion mutants of *crb::mEosFP^{KI}*. Two *crb::mEosFP^{KI}* donor DNA fragments were recombined into the *crb* locus as a tandem-dimmer. Such tandem-insertion mutants still retained *UAS-Rpr*, but they could not be distinguished from standard targeting events by the PCR#1 in **a**.

c. PCR verification of the tandem-insertion in *crb::mEosFP^{KI}* targeting candidates #9 and #14. The PCR flanks the junction region between two tandem insertions that contain *UAS-Rpr*. *crb::mEosFP^{KI}* mutant #2 was used as a control. #9 and #14 showed strong PCR products of expected size. A very faint PCR product can be seen in the #2 sample, but it is non-specific since it is smaller than the expected size. WT: *w^{1118}* wild type. MW: molecular weight marker (Invitrogen 1kb-plus).

d. Wing inflation phenotype in a *P{pRK1-crb::mEosFP$^{KI\#3A}$}/+; Gal4^{221}/+* adult escaper.

Supplementary Figure 2. Generation and verification of *dArf6^{KO}* mutants.

a. Diagnostic PCR screens of *dArf6^{KO}* candidates on the 2nd chromosome. All three “deletion-PCRs” in **b** and **c** were designed to be located within the targeted deletion of *dArf6* (dashed bar in Fig. 2c), while the control-PCR was designed to be located in the 5’ gDNA region (Fig. 2c). Deletion-PCR#2 (273bp) and control-PCR (534b) were used to screen homozygous males from each of the 2nd chromosome candidates. For each candidate, both PCR samples were loaded together on the gel.

b. PCR verification of *dArf6^{KO}* candidates. #2, 3, 16, 25 and 27 were specific targeting candidates that were negative in all three deletion-PCRs. #5 was a non-specific candidate that served as a control. For each candidate, both deletion-PCR and control-PCR samples were loaded together on the gel. *donor*: transgenic donor line pRK2-dArf6$^{KO\#13}$. *{7/16}*: since candidate #7 apparently harbored a background lethal mutation, it was screened as trans-heterozygote *dArf6$^{KO\#7}$/dArf6$^{KO\#16}$*.

In both **a** and **b**, arrows are pointing to control-PCR products (534bp), while arrowheads are pointing to deletion-PCR products.

Supplementary Table 1. Published *Drosophila* mutants that were generated by ends-out targeting.*

Gene	Targeted Deletion	5' + 3' Arms (kb)	HR Freq.	Reference
G9a	*n/a*	*n/a*	*n/a*	(SEUM *et al.* 2007a)
Snmp	~2.4kb	5 + 5	$3x10^{-5}$	(BENTON *et al.* 2007)
cry	~3 kb	2.9 + 2.8	*n/a*	(DOLEZELOVA *et al.* 2007)
miR-8	400bp	3 + 3	*n/a*	(KARRES *et al.* 2007)
DmSetdb1	~2.5kb	4.1 + 3.9	*n/a*	(SEUM *et al.* 2007b)
elmo	2.062kb	*n/a*	*n/a*	(BIANCO *et al.* 2007)
Dscam2	1.8kb	3.5 + 3.1	*n/a*	(MILLARD *et al.* 2007)
nautilus	armGFP	2.9 + 5.3	*n/a*	(WEI *et al.* 2007)
loqs	~2kb	4.4 + 2.3	$3.9x10^{-4}$	(PARK *et al.* 2007)
Gr63a	~1.7kb	2.8 + 3.9	$3.3x10^{-6}$	(JONES *et al.* 2007)
Obp57d ***Obp57e*** ***Obp57d/e***	~0.34kb ~0.45kb ~1.3kb	*2.8+3.4* *3.6+2.5* *2.8+2.5*	*n/a*	(MATSUO *et al.* 2007)
Sra	1.18kb	3.0+2.4	*n/a*	(TAKEO *et al.* 2006)
dpis	~500bp	3.0 + 3.3	*n/a*	(WANG and MONTELL 2006)
miR-9a	78bp	4.2 + 4.7	*n/a*	(LI *et al.* 2006)
hib	2.5kb	4 + 4	*n/a*	(ZHANG *et al.* 2006)
csk	5.5kb	*n/a*	*n/a*	(O'REILLY *et al.* 2006)
dSfmbt	54bp	3.3 + 3.3	*n/a*	(KLYMENKO *et al.* 2006)
Hand	~4kb	2.5 + 3.1	$3x10^{-4}$	(HAN *et al.* 2006)
miR-278	160bp	3.6 + 3.6	*n/a*	(TELEMAN *et al.* 2006)
ry	0bp	4.16 (total)	$> \sim 10^{-4}$	(BEUMER *et al.* 2006)
CG14517	200bp	3+3	$2x10^{-4}$** $5x10^{-5}$** $3.3x10^{-5}$**	(HAINES and IRVINE 2005)
WntD	22bp	3+3	*n/a*	(GORDON *et al.* 2005)
yorkie	~2kb	4 + 4	*n/a*	(HUANG *et al.* 2005)
fruitless	Gal4 Knok-In	3 + 3	$5.3x10^{-3}$	(MANOLI *et al.* 2005)
hsp70A ***hsp70Ba*** ***hsp70B***	5.85kb 1.73kb 46.7kb	3.7 + 3.6 4.3 + 4.1 5.1 + 4.5	$5x10^{-5}$ $5x10^{-5}$ $2x10^{-5}$	(GONG and GOLIC 2004)
Or83b	~3kb	6.5 + 3.7	*n/a*	(LARSSON *et al.* 2004)
dMrtf	~5kb	4 + 4	$8x10^{-5}$	(HAN *et al.* 2004)
mre11	~2kb	*n/a*	*n/a*	(BI *et al.* 2004)

5' + 3' Arms: the sizes of 5' and 3' homologous DNA arms in the targeting construct.
HR: Homologous Recombination.

*: Based on the citation record of the original ends-out targeting paper by Gong & Golic 2003[1] from ISI Web of Knowledge (http://www.isiwebofknowledge.com).

**: Three different transgenic donor lines were used for CG14517 targeting experiments, with HR frequency of 1/5000 ($2x10^{-4}$),1/20000 ($5x10^{-5}$) and 1/30000 ($3.3x10^{-5}$), respectively.

Supplementary Table 2. Validating the integrity of the pRK1 and pRK2 vectors

Targeting Constructs	Transgenic Lines	Chr. Insertion	×*Gal4*^{477} [a]	×*Gal4*^{221} [a]	×*hs-FLP* [b]	×*hs-Cre* [b]
pRK1-crb::mEosFP^{KI}	1B	*3*rd	lethal	*n/d*	~50%	100%
	2A	*3*rd	lethal	*n/d*	~40%	100%
	3A [c]	*2*nd	lethal	lethal	~50%	100%
	4B	*3*rd	lethal	*n/d*	~70%	100%
	5B	*3*rd	lethal	*n/d*	~70%	100%
	6A	*2*nd	lethal	*n/d*	~40%	100%
	8	*3*rd	lethal	*n/d*	~70%	100%
	9A	*3*rd	lethal	*n/d*	~60%	100%
	10B	*3*rd	lethal	*n/d*	~60%	100%
pRK2-dArf6^{KO}	1	*2*nd	*n/d*	lethal	~10%	100%
	2	*2*nd	*n/d*	lethal	*n/d*	100%
	3 [d]	*2*nd	*n/d*	lethal	0%	0%
	4	*3*rd	*n/d*	lethal	~10%	100%
	5 [d]	*2*nd	*n/d*	lethal	0%	0%
	6	*2*nd	*n/d*	lethal	~5%	100%
	7	*2*nd	*n/d*	lethal	~30%	100%
	8	*3*rd	*n/d*	lethal	~10%	100%
	9	*2*nd	*n/d*	lethal	~50%	100%
	10	*3*rd	*n/d*	lethal	~10%	100%
	11	*2*nd	*n/d*	lethal	~20%	100%
	12	*2*nd	*n/d*	lethal	~10%	100%
	13 [c]	*3*rd	*n/d*	lethal	~15%	100%
	14	*2*nd	*n/d*	lethal	~20%	100%
	15	*2*nd	*n/d*	lethal	~10%	100%
	16	*2*nd	*n/d*	lethal	~20%	100%
[e]*pUAST-Baz::mEosFP*	1A	*n/d*	viable	*n/d*	0%	0%

a. *Gal4*^{477}*/UAS-Rpr* larvae were mostly arrested at the 3rd instar stage, a few developed to pupation, but none of them matured to adults. A majority of *Gal4*^{221}*/UAS-Rpr* larvae and pupae were lethal, with a few adult escapers showing a strong wing inflation phenotype (Supplementary Fig. 1d).

b. These tests validated the FRT and loxP sites in the pRK1 and pRK2 vectors. In *hs-FLP* and *hs-Cre* crosses, the degree of eye color variegation due to loss of w^+ was compared by estimating the percentage of white area in each eye. *hs-FLP* and *hs-Cre* stocks used here constitutively express FLPase or Cre recombinase. pRK2-dArf6^{KO} scored lower than pRK1-Crb::mEosFP in the FLPase-induced eye color variegation test. This is most likely due to the fact that the GMR enhancer in the pRK2 vector drives very strong expression of w^+, so cells with late or partial loss of w^+ still retain highly visible color.

c: These two lines were used for *crb::mEosFP*^{KI} and *dArf6*^{KO} targeting experiments, respectively.

d. Donor DNA fragment in these two lines were likely damaged during P-element based transgenesis.

e. This line was included as a negative control. It is based on the common pUAST vector that contains no FRT and loxP sites.

SUPPLEMENTARY REFERENCES:

BENTON, R., K. S. VANNICE and L. B. VOSSHALL, 2007 An essential role for a CD36-related receptor in pheromone detection in Drosophila. Nature 450: 289-293.

BEUMER, K., G. BHATTACHARYYA, M. BIBIKOVA, J. K. TRAUTMAN and D. CARROLL, 2006 Efficient Gene Targeting in Drosophila With Zinc-Finger Nucleases. Genetics 172: 2391-2403.

BI, X., S. C. WEI and Y. S. RONG, 2004 Telomere protection without a telomerase; the role of ATM and Mre11 in Drosophila telomere maintenance. Curr Biol 14: 1348-1353.

BIANCO, A., M. POUKKULA, A. CLIFFE, J. MATHIEU, C. M. LUQUE *et al.*, 2007 Two distinct modes of guidance signalling during collective migration of border cells. Nature 448: 362-365.

DOLEZELOVA, E., D. DOLEZEL and J. C. HALL, 2007 Rhythm defects caused by newly engineered null mutations in Drosophila's cryptochrome gene. Genetics 177: 329-345.

GONG, W. J., and K. G. GOLIC, 2003 Ends-out, or replacement, gene targeting in Drosophila. Proc Natl Acad Sci U S A 100: 2556-2561.

GONG, W. J., and K. G. GOLIC, 2004 Genomic deletions of the Drosophila melanogaster Hsp70 genes. Genetics 168: 1467-1476.

GORDON, M. D., M. S. DIONNE, D. S. SCHNEIDER and R. NUSSE, 2005 WntD is a feedback inhibitor of Dorsal/NF-[kappa]B in Drosophila development and immunity. Nature 437: 746-749.

GRUEBER, W. B., L. Y. JAN and Y. N. JAN, 2003 Different levels of the homeodomain protein cut regulate distinct dendrite branching patterns of Drosophila multidendritic neurons. Cell 112: 805-818.

HAINES, N., and K. D. IRVINE, 2005 Functional analysis of Drosophila {beta}1,4-N-acetlygalactosaminyltransferases. Glycobiology 15: 335-346.

HAN, Z., X. LI, J. WU and E. N. OLSON, 2004 A myocardin-related transcription factor regulates activity of serum response factor in Drosophila. Proc Natl Acad Sci U S A 101: 12567-12572.

HAN, Z., P. YI, X. LI and E. N. OLSON, 2006 Hand, an evolutionarily conserved bHLH transcription factor required for Drosophila cardiogenesis and hematopoiesis. Development 133: 1175-1182.

HAY, B. A., T. WOLFF and G. M. RUBIN, 1994 Expression of baculovirus P35 prevents cell death in Drosophila. Development 120: 2121-2129.

HUANG, J., S. WU, J. BARRERA, K. MATTHEWS and D. PAN, 2005 The Hippo signaling pathway coordinately regulates cell proliferation and apoptosis by inactivating Yorkie, the Drosophila Homolog of YAP. Cell 122: 421-434.

JONES, W. D., P. CAYIRLIOGLU, I. G. KADOW and L. B. VOSSHALL, 2007 Two chemosensory receptors together mediate carbon dioxide detection in Drosophila. Nature 445: 86-90.

KARRES, J. S., V. HILGERS, I. CARRERA, J. TREISMAN and S. M. COHEN, 2007 The conserved microRNA miR-8 tunes atrophin levels to prevent neurodegeneration in Drosophila. Cell 131: 136-145.

KLYMENKO, T., B. PAPP, W. FISCHLE, T. KOCHER, M. SCHELDER *et al.*, 2006 A Polycomb group protein complex with sequence-specific DNA-binding and selective methyl-lysine-binding activities. Genes Dev 20: 1110-1122.

LARSSON, M. C., A. I. DOMINGOS, W. D. JONES, M. E. CHIAPPE, H. AMREIN *et al.*, 2004 Or83b encodes a broadly expressed odorant receptor essential for Drosophila olfaction. Neuron 43: 703-714.

LI, Y., F. WANG, J. A. LEE and F. B. GAO, 2006 MicroRNA-9a ensures the precise specification of sensory organ precursors in Drosophila. Genes Dev 20: 2793-2805.

MANOLI, D. S., M. FOSS, A. VILLELLA, B. J. TAYLOR, J. C. HALL *et al.*, 2005 Male-specific fruitless specifies the neural substrates of Drosophila courtship behaviour. Nature 436: 395-400.

MATSUO, T., S. SUGAYA, J. YASUKAWA, T. AIGAKI and Y. FUYAMA, 2007 Odorant-Binding Proteins OBP57d and OBP57e Affect Taste Perception and Host-Plant Preference in Drosophila sechellia. PLoS Biol 5: e118.

MILLARD, S. S., J. J. FLANAGAN, K. S. PAPPU, W. WU and S. L. ZIPURSKY, 2007 Dscam2 mediates axonal tiling in the Drosophila visual system. Nature 447: 720-724.

O'REILLY, A. M., A. C. BALLEW, B. MIYAZAWA, H. STOCKER, E. HAFEN *et al.*, 2006 Csk differentially regulates Src64 during distinct morphological events in Drosophila germ cells. Development 133: 2627-2638.

PARK, J. K., X. LIU, T. J. STRAUSS, D. M. MCKEARIN and Q. LIU, 2007 The miRNA pathway intrinsically controls self-renewal of Drosophila germline stem cells. Curr Biol 17: 533-538.

SEUM, C., S. BONTRON, E. REO, M. DELATTRE and P. SPIERER, 2007a Drosophila G9a Is a Nonessential Gene. Genetics 177: 1955-1957.

SEUM, C., E. REO, H. PENG, F. J. RAUSCHER, 3RD, P. SPIERER *et al.*, 2007b Drosophila SETDB1 is required for chromosome 4 silencing. PLoS Genet 3: e76.

TAKEO, S., M. TSUDA, S. AKAHORI, T. MATSUO and T. AIGAKI, 2006 The Calcineurin Regulator Sra Plays an Essential Role in Female Meiosis in Drosophila. Current Biology 16: 1435-1440.

TELEMAN, A. A., S. MAITRA and S. M. COHEN, 2006 Drosophila lacking microRNA miR-278 are defective in energy homeostasis. Genes Dev 20: 417-422.

WANG, T., and C. MONTELL, 2006 A phosphoinositide synthase required for a sustained light response. J Neurosci 26: 12816-12825.

WEI, Q., Y. RONG and B. M. PATERSON, 2007 Stereotypic founder cell patterning and embryonic muscle formation in Drosophila require nautilus (MyoD) gene function. Proc Natl Acad Sci U S A 104: 5461-5466.

WIEDENMANN, J., S. IVANCHENKO, F. OSWALD, F. SCHMITT, C. ROCKER *et al.*, 2004 EosFP, a fluorescent marker protein with UV-inducible green-to-red fluorescence conversion. Proc Natl Acad Sci U S A 101: 15905-15910.

WODARZ, A., U. HINZ, M. ENGELBERT and E. KNUST, 1995 Expression of crumbs confers apical character on plasma membrane domains of ectodermal epithelia of Drosophila. Cell 82: 67-76.

ZHANG, Q., L. ZHANG, B. WANG, C. Y. OU, C. T. CHIEN *et al.*, 2006 A hedgehog-induced BTB protein modulates hedgehog signaling by degrading Ci/Gli transcription factor. Dev Cell 10: 719-729.

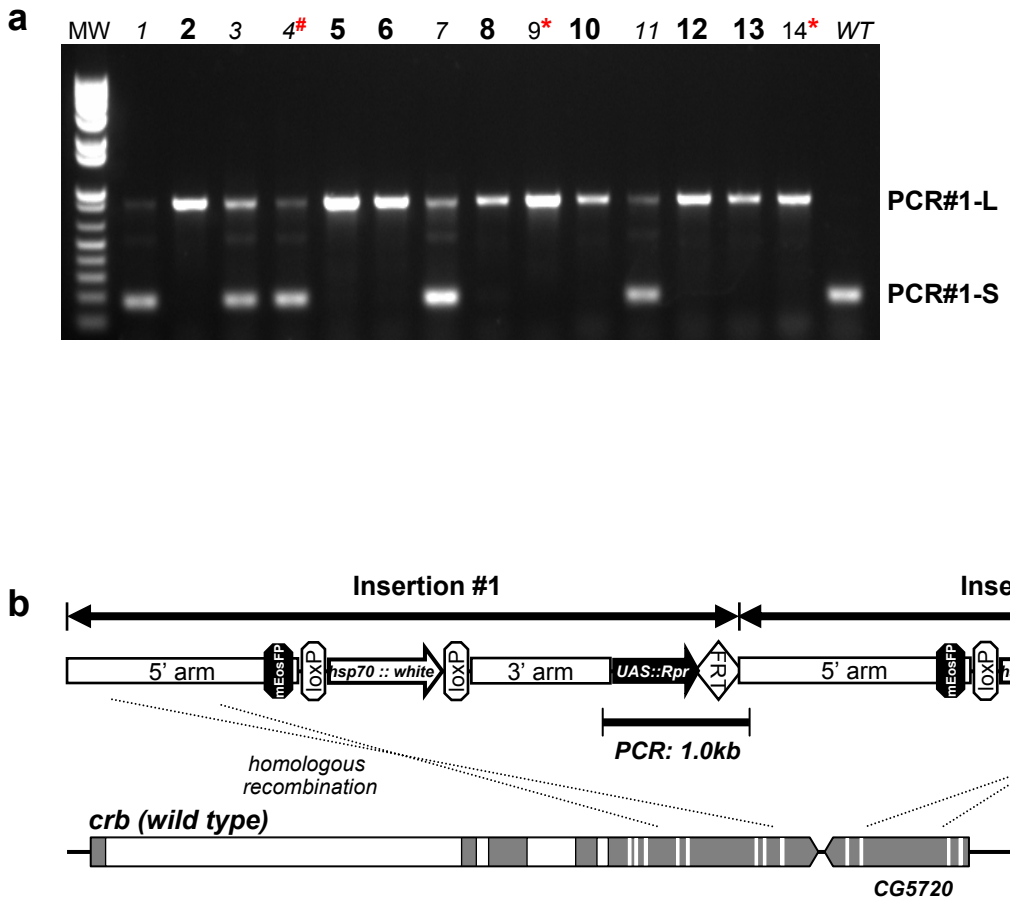

J. Huang & Y. Hong **Supplementary Figure 1**

a

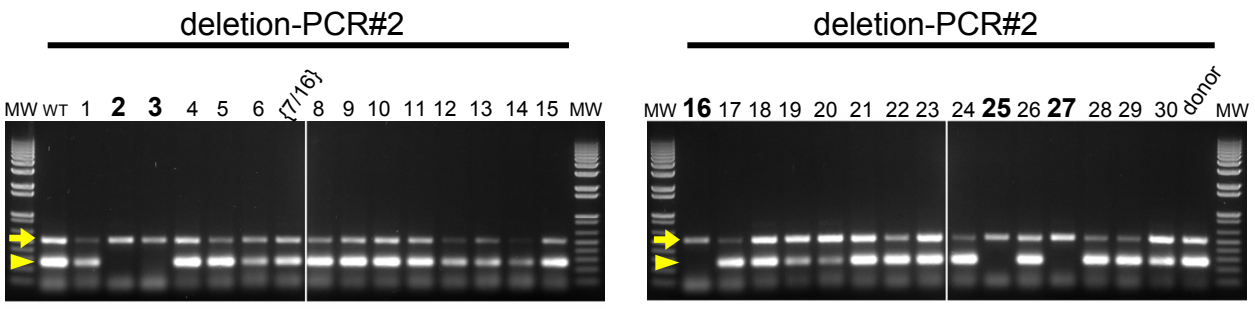

b

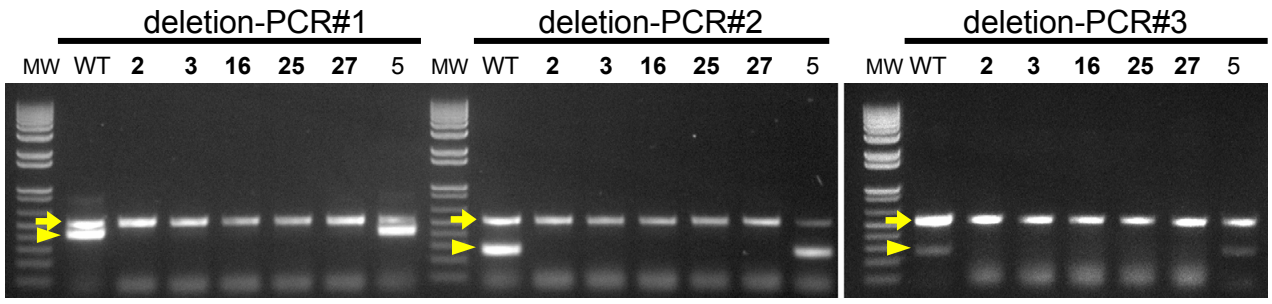

J. Huang & Y. Hong **Supplementary Figure 2**